Modeling and Experimental Validation of In-Plane Wheel Vibrations due to Tire Non-uniformity

Z. Liu[1], K. Sepahvand[1], Y. T. Wei[2], S. Marburg[1]

[1] *Department of Mechanical Engineering, Technical University of Munich, 85748 Garching, Germany, E-Mail: zhe.liu@tum.de*

[2] *Department of Automotive Engineering, State Key Lab Automotive Safety and Energy, Tsinghua University, Beijing, 100084, China*

Introduction

Tire non-uniformities give rise to the force variations at the spindle during the steady-state rotation. The higher-order harmonics of the axial forces caused by the tire uniformity subsequently induce the noise within passenger cars. Considering the complicated production process of tires, it is inevitable to cause uncertainties in tire structures. The defects of tires, such as the unbalanced mass distribution and the uneven radial run-out will result in the variation of the dynamic response of tires.

The non-uniformity of tires has been reported in several published studies to be the major causes of the riding discomfort [1-2]. Walker and Reeves have discussed the mechanism of the deviation of the axial forces based on the experimental results [3]. Based on the assumption of the rigid ring, Stutts *et al*. have explained the phenomenon that the horizontal force increases faster than the vertical forces as the speed increases [4]. The influences of the lamped stiffness of the sidewall have been studied subsequently [5]. Dillinger *et al*. have combined some published models of tires and analyzed the tangential and radial hub forces [6]. Pottinger has summarized the methods to improve the response of the installed non-uniform tire-wheel assemblies. [7]. However, most of the researches have focused on the explanation of experimental results [3-4, 7]. Some existing models which have applied the assumption of the rigid ring are too simple to describe the tire deformation and the behaviors in the tire-road contact area [4-6]. Therefore, the purpose of this paper is to develop a model for predicting the force transmissibility of tires caused by the non-uniformity, including the mass unbalance and the radial run-out. The model is established based on a flexible-rigid ring model. The impacts of these two kinds of non-uniformities are analyzed at different speeds.

Ring Model of Tire

A method of transforming a pneumatic tire into a ring model has been widely used in the analysis of vehicle dynamics. To analyze the in-plane dynamic response of tires, a tire was modeled as a two-dimensional deformable ring in this paper. It means that only the motions in the plane of the wheel were considered [8-9].

2D Ring Model

Herein, the steel belt is treated as a 2D elastic ring. It is assumed as an Euler-Bernoulli beam which can bend in the plane of the wheel. The sidewall is equivalent to an elastic foundation with damping, and the rim is rigid. Figure 1 shows the method of transforming a tire into a 2D deformable ring with a rectangular cross-section on an elastic foundation. The location of any point on the tire can be described by cylindrical coordinates in the non-rotating coordinate system (r, θ), or the rotating coordinate system (r, ϕ). The uniform pressure was applied to the inner wall. The elastic properties of the elastic foundation are modeled respectively by distributed springs in the radial and circumferential directions (k_u, k_v). Damping existing in the foundation can be described by introducing the coefficients (c_u, c_v) into this model.

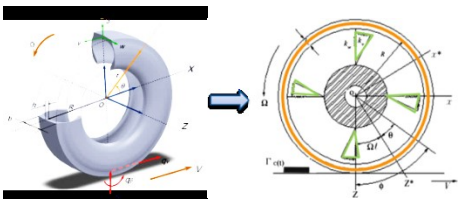

Figure 1: Schematic of the two-dimensional ring model of tires.

The radial and circumferential displacements (u, v) are applied to describe the motion of the ring, which can be expressed by the mid-plane displacements (u_b, v_b). The tread band is assumed to behave as an inextensible curved beam. Therefore, the radial displacement u and the tangential displacement v at any point on the middle surface of the inextensible ring are related by

$$u_b = -v_b' \tag{1}$$

The equation of motion of the ring expressed in terms of v_b is given in [8]. The response of the tangential displacement of the ring is expressed in terms of a modal expansion. The motion in the generalized coordinates $a_n(t)$, $b_n(t)$ reduces to a set of linear second-order ordinary differential equations

$$\begin{bmatrix} m_n & 0 \\ 0 & m_n \end{bmatrix} \begin{Bmatrix} \ddot{a}_n \\ \ddot{b}_n \end{Bmatrix} + \begin{bmatrix} \cdots & \cdots \\ \cdots & \cdots \end{bmatrix} \begin{Bmatrix} \dot{a}_n \\ \dot{b}_n \end{Bmatrix} + \begin{bmatrix} \cdots & \cdots \\ \cdots & \cdots \end{bmatrix} \begin{Bmatrix} a_n \\ b_n \end{Bmatrix} = \begin{Bmatrix} \xi_n \\ \eta_n \end{Bmatrix}. \tag{2}$$

The elements in the matrices are as follows

$$\begin{aligned} & m_n = \rho A\left(1+n^2\right); \quad g_n = -4\rho A n\Omega; \quad c_n = c_v + c_w n^2 \\ & k_n = \left(\frac{EI}{R^4}n^2 + \frac{\sigma_\varepsilon^0 A}{R^2}\right)\left(1-n^2\right)^2 - \frac{p_0 b}{R}\left(1-n^2\right) + k_v + k_w n^2 - \rho A\left(1+n^2\right)\Omega^2 \end{aligned}, \tag{3}$$

where σ_ε^0 is the initial stress in the tread band due to the action of the centrifugal force and inflation pressure p_0. With

the case of concentrated line forces and moment (q_u, q_v, q_β) acting on the tread, the steady-state response is obtained using the undetermined coefficient method,

$$\begin{aligned} q_u(\theta,t) &= Q_u\delta(\phi-\phi_0) = Q_u\delta\left(\theta-(\phi_0-\Omega t)\right) \\ q_v(\theta,t) &= Q_v\delta(\phi-\phi_0) = Q_v\delta\left(\theta-(\phi_0-\Omega t)\right) \\ q_\beta(\theta,t) &= Q_\beta\delta(\phi-\phi_0) = Q_\beta\delta\left(\theta-(\phi_0-\Omega t)\right) \end{aligned}, \tag{4}$$

where Q_u, Q_v, and Q_β, are the magnitudes of radial and tangential forces and the moment acting at specified point ϕ_0 in the non-rotating coordinates. If the ring is discretized, the overall displacement of the tread band can be obtained by the superposition of the response at each point. The tangential displacement and the corresponding radial displacement of the tread band are given by

$$\begin{aligned} v_b(\phi,t) &= \sum_{k=1}^{kc}\sum_{n=1}^{\infty}\begin{bmatrix} \bar{A}_{n1}\left(Q_{vk}+\left(1-n^2\right)Q_{\beta k}\right)\cos n\left(\phi_0-\phi+\gamma_n\right) \\ +\bar{A}_{n2}Q_{uk}\sin n\left(\phi_0-\phi+\gamma_n\right)\end{bmatrix} \\ u_b(\phi,t) &= \sum_{k=1}^{kc}\sum_{n=1}^{\infty}\begin{bmatrix} -n\bar{A}_{n1}\left(Q_{vk}+\left(1-n^2\right)Q_{\beta k}\right)\sin n\left(\phi_0-\phi+\gamma_n\right) \\ +n\bar{A}_{n2}Q_{uk}\cos n\left(\phi_0-\phi+\gamma_n\right)\end{bmatrix} \end{aligned} \tag{5}$$

where

$$\begin{aligned} &\bar{A}_{n1} = \frac{1}{\pi\sqrt{\left(\bar{M}_n-\bar{G}_n\right)^2+\left(\bar{C}_n\right)^2}};\ n\gamma_n = \arctan\left(\frac{\bar{C}_n}{\bar{M}_n-\bar{G}_n}\right); \\ &\bar{A}_{n2} = n\bar{A}_{n1};\bar{M}_n = k_n-(n\Omega)^2m_n;\bar{G}_n = (n\Omega)g_n;\bar{C}_n = (n\Omega)c_n \end{aligned} \tag{6}$$

Equation (5) also can be transformed into a matrix form,

$$\mathbf{U} = \mathbf{TQ}, \tag{7}$$

where **U** is the displacements of tire body, **T** is the flexibility matrix, **Q** is the matrix of generalized forces. Once the forces and moment (q_u, q_v, q_β) acting on the tread band are given, the tire tread band displacements (u_b, v_b) can be obtained from equation (7).

Contact Forces

The displacements of the tire body cannot be calculated in advance, because the tire body is not directly in contact with the road surface. The displacements of the tire body and the tread rubber should be satisfied with the geometry compatible conditions [10]. The rotation angle β of the tread band cross-section is

$$\beta = \frac{v_b-u_b'}{R}. \tag{8}$$

Under a given overall deformation, the normal and tangential deformations of the tread rubber (u_s, v_s), and The declination η and the rotation angle β of the tread band cross-section at any given position ϕ are expressed as

$$\begin{aligned} u_s &= R_l\cos\eta + R_e\phi\sin\eta - (R+u_b)\cos\beta - v_b\sin\beta \\ v_s &= -R_l\sin\eta + R_e\phi\cos\eta + (R+u_b)\sin\beta - v_b\cos\beta \\ \eta &= \phi+\beta \end{aligned}. \tag{9}$$

The forces acting on the rubber surface can be calculated as

$$\begin{aligned} F_{ns} &= k_{Es}(u_s-h_0) \\ F_{ts} &= k_{Gs}v_s \end{aligned}. \tag{10}$$

The generalized forces and the tractions are obtained by using the coordination transformation,

$$\begin{Bmatrix} q_u(\phi) \\ q_v(\phi) \\ q_\beta(\phi)\end{Bmatrix} = \begin{bmatrix} \cos\beta & -\sin\beta \\ \sin\beta & \cos\beta \\ 0 & u_s\end{bmatrix}\begin{Bmatrix} F_{ns}(\phi) \\ F_{ts}(\phi)\end{Bmatrix}, \tag{11}$$

$$\begin{Bmatrix} \sigma \\ \tau\end{Bmatrix} = \begin{bmatrix} \cos\eta & -\sin\eta \\ \sin\eta & \cos\eta\end{bmatrix}\begin{Bmatrix} F_{ns} \\ F_{ts}\end{Bmatrix}. \tag{12}$$

Assuming the displacements of the tire body are small. Substituting the equations (9-10) into the equation (11) and transforming to the matrix form, the linearized boundary equation is,

$$\mathbf{Q} = \mathbf{F} + \mathbf{HU}, \tag{13}$$

where **F** is the matrix of generalized forces corresponding to the tread rubber deformation. The exact contact forces are obtained by successive substitution which is treated as the input of the rigid ring to calculate the transient responses.

Flexible-rigid Coupling Ring

Solving the partial differential equations of the tire motion considering the large-deformation and the rotation will make the dynamic model too complex to solve. Therefore, the transient response can be approximated using an assumption of the rigid ring to describe the first modes of the tire body (<100Hz). The rigid ring can represent the inertia of the tread and a part of the sidewall. The rigid ring is connected to the rim by a three degrees-of-freedom spring element. To calculate the transient response, the contact forces generated by the flexible ring are treated as the input excitation on the rigid ring. Then the position will be frozen to calculate the local deformation and the next-step contact forces.

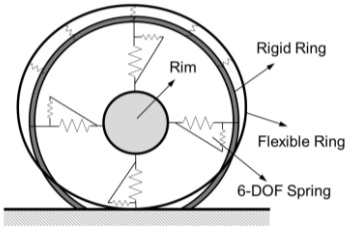

Figure 2: Combination of the flexible ring and the rigid ring.

Non-uniformity Parameters

In this paper, two kinds of non-uniformities of the tire are considered, including the lumped mass unbalance and the geometrical radial run-out. These non-uniformities not only affect the parameter matrixes in the flexible ring model but also influence the contact forces and the dynamic response. The concentrated mass unbalance is described in the equations of motion of the rigid ring. It causes the additional generalized forces in the system. The effects were discussed in the section of the simulation results.

Model Parameter

To demonstrate the validity of this proposed model, a practical tire structure was modeled in this paper. As in the case study, the proposed ring model is applied to the non-uniformity analysis of a 205/55R16 radial tire. Some engineering design parameters are listed in Table 1.

Table 1: Geometrical parameters of a 205/55R16 tire

Parameter type	Unit	Value
Ring width b	m	0.172
Ring thickness h	m	0.018
Effective density ρ	kg/m^3	1.6×10^3
Mean radius R	m	0.32
Inflation pressure p_0	Pa	2.4×10^5

The parameters of the flexible ring model including the geometric and physical parameters are identified from the results of the finite element model. The parameters of the rigid ring and the stiffness parameters of the 3-DOF spring are obtained by using the results of the first-order natural frequencies. Those parameters also can be obtained from cleat tests or static stiffness experiments [11].

Table 2: Physical parameters of the flexible ring

Parameter type	Unit	Value
In-plane bending stiffness EI	N m^2	2.0
Radial distributed springs of sidewall k_u	N/m^2	6.3×10^5
Circumferential distributed springs of sidewall k_v	N/m^2	1.89×10^5
Tread band thickness h_0	m	0.0125
Tread normal stiffness k_{Es}	N/m	3.3×10^5
Tread tangential stiffness k_{Gs}	N/m	3.93×10^5

Table 3: Physical parameters of the rigid ring

Parameter type	Unit	Value
Mass of the rigid ring	kg	6.9
Horizontal stiffness of the spring	N/m	1.7×10^6
Vertical stiffness of the spring	N/m	1.04×10^6
Torsional stiffness of the spring	N/rad	2.72×10^3

Simulation Results

Contact Pressure Distribution

The results of the contact force distribution under five different vertical load conditions are shown in Fig. 3. At the center part of the contact patch, the concave distribution under a higher vertical load illustrates a trend of buckling.

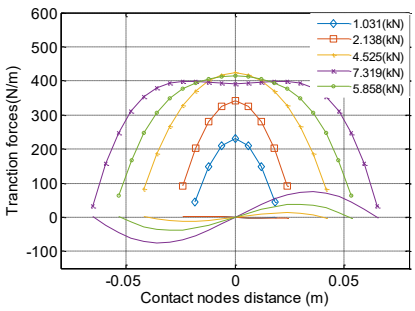

Figure 3: Results of the contact force distribution.

Responses Caused by Radial Run-out

A set of test data of the radial run-out at the center point (RRoc) on the outer surface of the tire is given. To simulate the experimental conditions, the height of the spindle is fixed. Without the mass unbalance, the radial force deviation per revolution is given in Figure 4.

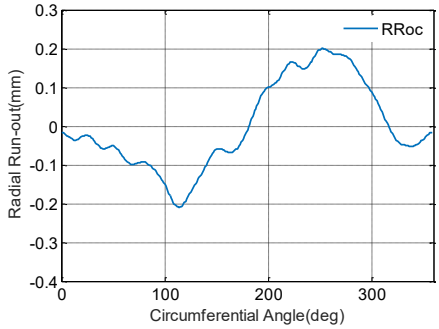

(a) Radial run-out test data at the center point of the tire

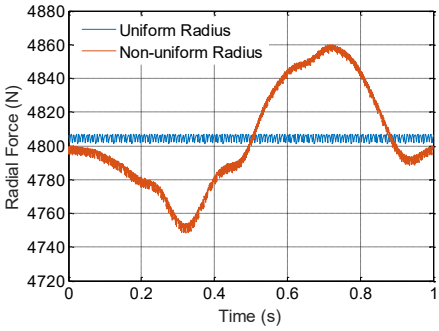

(b) Radial force deviation per revolution

Figure 4: Radial force of the tire caused by the radial run-out of at the center point on the outer tread band surface.

Responses Caused by Mass Unbalance

As the rolling speed of the tire increases, the horizontal force increases faster than the vertical force [3]. In this case study, the effects on the force deviation caused by a concentrated unbalanced mass on the tread m_a were analyzed. Assume that it is possible to place a counterbalancing mass m_c at the rim which satisfies the condition, $m_a R_e = m_c R_c$, where R_c is the radius of the rim.

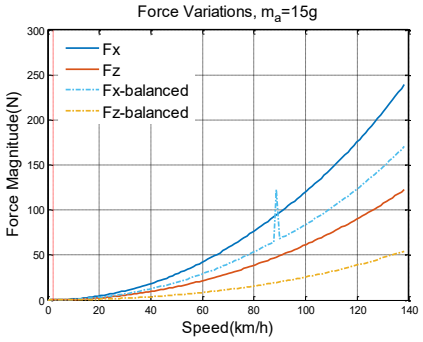

Figure 5: Deviation of the vertical and horizontal forces of the unbalanced and counterbalanced systems.

Figure 5 shows the results of the unbalanced and counterbalanced systems where the unbalanced mass $m_a = 15$ g was selected. It is found that the horizontal force is

larger. The effect of the mass unbalance cannot be completed omitted by the counterbalanced mass on the rim, and the resonance of the rim is observed in the responses of the balanced horizontal force.

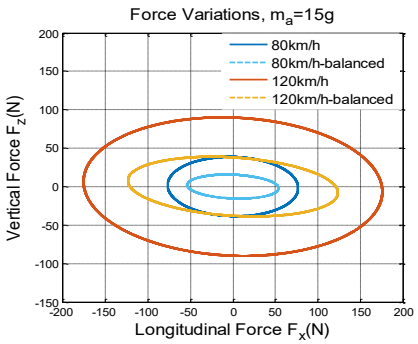

Figure 6: Diagram of the vertical and horizontal forces at the rolling speed of 80 km/h and 120 km/h.

For the unbalanced and counterbalanced systems, the diagram of the vertical and horizontal forces at the rolling speed of 80 km/h and 120 km/h are given in Fig. 6. The horizontal force dominates at different rolling speeds.

Dynamic Simulation

To investigate the impacts of the run-out and the mass unbalance on the responses, the practical RRoc is simplified as a trigonometric function, $y = Y_e \cos(\Omega t - \delta)$, where δ represents the location of the maximum amplitude of the run-out relative to the rotating frame. Here the amplitude Y_e equals to 0.2mm and δ is chosen as 0.

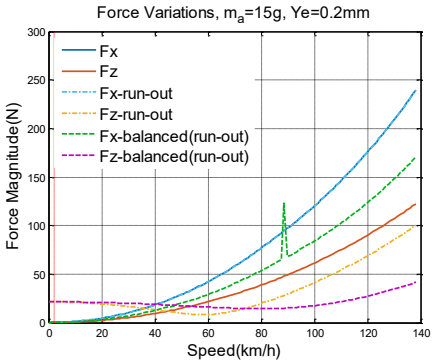

Figure 7: Schematic of the three-dimensional ring model.

At low rolling speed, the vertical force is larger, but at high rolling speed, the horizontal force dominates as shown in Fig.7. It means that even if the low-speed test results of tires meet the production requirements, the force deviations caused by the mass unbalance will be significant at high speed, especially in the horizontal direction.

Conclusion

In this paper, a multi-body model for analyzing the characteristics of the force transmissibility of a non-uniform tire was proposed. Tire non-uniformities give rise to rolling force variation on the spindle during steady-state rolling. The impacts of the mass unbalance and the radial run-out were investigated by the proposed flexible-rigid ring model which was established based on a three-dimensional ring on an elastic foundation model. Considering the geometric non-uniformity of the tire, the variations of the vertical force in the tire-road contacting area were given. The horizontal and vertical forces caused by the mass unbalance and the radial run-out were calculated. It shows that the effect of the mass unbalance cannot be completed omitted by the counterbalanced mass on the rim, and the resonance of the rim will be involved in the force responses. By simplifying the radial run-out as a trigonometric function, it is observed that as the horizontal force deviations caused by the mass unbalance dominates at high speed.

Acknowledgment

The first author acknowledges the support from the China Scholarship Council (CSC).

Reference

[1] Clark, S. K. The rolling tire under load. SAE Technical Paper No. 650493, (1965).

[2] Clarke, S. K. Mechanics of pneumatic tyres. United States Department of Commerce, National Bureau of Standards (1971).

[3] Walker, J. C., and N. H. Reeves. Uniformity of tires at vehicle operating speeds. Tire Science and Technology 2.3 (1974): 163-178.

[4] Stutts, D. S., W. Soedel, and S. K. Jha. Fore-aft Forces in Tire-Wheel Assemblies Generated by Unbalances and the Influence of Balancing. Tire Science and Technology 19.3 (1991): 142-162.

[5] Stutts, D. S., C. M. Krousgrill, and W. Soedel. Parametric excitation of tire-wheel assemblies by a stiffness non-uniformity. Journal of sound and vibration 179.3 (1995): 499-512.

[6] Dillinger, Brian L., Nader Jalili, and Imtiaz Ul Haque. Analytical modelling and experimental verification of tyre non-uniformity. International journal of vehicle design 46.1 (2008): 1-22.

[7] Pottinger, Marion G. Uniformity: A Crucial Attribute of Tire/Wheel Assemblies. Tire Science and Technology 38.1 (2010): 24-46.

[8] Wei Y.T., Nasdala L., Rothert H., Analysis of forced transient response for rotating tires using REF models, Journal of Sound and Vibration 320(2009) 145-162.

[9] Liu, Z, et al. Three-dimensional vibration of a ring with a noncircular cross-section on an elastic foundation. Proceedings of the Institution of Mechanical Engineers, Part C: Journal of Mechanical Engineering Science 232.13 (2018): 2381-2393.

[10] Kim, Son-Joo, and Arvin R. Savkoor. The contact problem of in-plane rolling of tires on a flat road. Vehicle System Dynamics 27.S1 (1997): 189-206.

[11] Kim, Seongho, Parviz E. Nikravesh, and Gwanghun Gim. A two-dimensional tire model on uneven roads for vehicle dynamic simulation. Vehicle system dynamics 46.10 (2008): 913-930.